Sequential Stack Decoder for Multichannel Image Restoration

Fouad Boudjenouia and Rachid Jennane
I3MTO Laboratory
Université d'Orléans, France
fouad.boudjenouia@etu.univ-orleans.fr
rachid.jennane@univ-orleans.fr

Karim Abed-Meraim and Aladine Chetouani
PRISME Laboratory, Polytech Orléans
Université d Orléans, France
karim.abed-meraim@univ-orleans.fr
aladine.chetouani@univ-orleans.fr

***Abstract*—In this paper, we propose a novel scheme for image restoration (IR) employing a sequential decoding technique based on a tree search, known as Stack algorithm. The latter is a well-known method used for 1D signal decoding in wireless communication systems. The main idea is to extend the Stack algorithm for image restoration (2D) and to exploit the information diversity conveyed by the channels (Multichannel) in order to restore the original image. To deal with the noisy case, a regularization term is introduced using the total variation and the wavelet transform. This method was tested on artificially degraded images (blurred and noisy). Obtained results confirm the relevance of the proposed approach.**

Keywords: Image restoration, Multichannel, Sequential decoding, Stack algorithm, Regularization.

I. Introduction

In this work we focus on applications where the recorded images are degraded forms of the initial scene due to flaws in the imaging and capturing process. It is vital to many of the subsequent image processing tasks to neutralize these flaws. One should consider an extensive variety of different degradations for example blur, noise, geometrical degradations, illumination and color imperfections [1] [2].

Image restoration (IR) from blurry and noisy observations is an important research field in image processing ranging from computer sciences, electronic engineering and remote sensing to medical and biology sciences. Image restoration from observations is a linear inverse problems that requires the determination of the unknown input to a linear system from the known output.

The IR is an ill-posed and ill-conditioned problem so it becomes necessary to take advantage of all kind of available information including the diversity gain associated with multichannel (MC) image processing. Preliminary results of multichannel deconvolution were first found in the one dimensional (1D) case, then extended to the two dimensional (2D) one. In the multichannel framework, several images are observed from a single scene that passes through different channels. Some applications where multichannel techniques could be used include: polarimetric, satellite, astronomical and microscopic imagery [3].

On the other hand, sequential decoding is a technique that was initially used in communication systems with noisy channels to restore transmitted signals using tree search algorithms. Several decoding methods exist in the literature including the Sphere Decoding (SD) [4] and the Stack algorithms [5]. The sphere decoding is an optimal lattice search technique but suffers from high computational complexity for large lattice dimension (which is the case in 2D image restoration problems). Alternatively, the Stack algorithm is an efficient and powerful tree search technique able to perform the desired signal decoding with a reduced complexity as compared to SD. Originally, the Stack algorithm was introduced as a low decoding complexity method for approximate maximum-likelihood (ML) signal estimation in communication systems.

In this paper, we use the Stack algorithm to achieve mono or multi-channel IR. At first, we show how the standard algorithm can be adapted and used properly in our context (2D). Then, to reduce further the computational cost, we introduce modified (faster) versions of the Stack algorithm by exploiting the 'band-limited' property of the filtering matrix together with a hierarchical decoding approach. Finally, to deal with the additive noise, we add appropriate regularization terms to the cost function and illustrate the overall algorithm's performance through numerical simulation experiments.

II. Problem Statement

In the case of multichannel systems, a single image passes through K independent channels ($K > 1$) leading to K noisy blurred images given by:

$$\begin{aligned} g_i(m,n) &= h_i(m,n) \star f(m,n) + w_i(m,n) \\ &= \sum_{l_1=0}^{m_h-1} \sum_{l_2=0}^{n_h-1} h_i(l_1,l_2)\, f(m-l_1,n-l_2) + w_i(m,n) \end{aligned} \tag{1}$$

for $m = 1,\cdots,m_g$ and $n = 1,\cdots,n_g$, where $\boldsymbol{f}$ denotes the source image and $\boldsymbol{g}_i$, $\boldsymbol{w}_i$, $\boldsymbol{h}_i$ for $i = 1,\cdots,K$, denote the observed images, noise matrices and point spread functions (PSF)[1], respectively. The latter filters are assumed known (or a priori estimated) and different enough to satisfy the diversity condition in [6]. By vectorizing the above matrices and stacking them into a single vector, we obtain:

$$\boldsymbol{g} = [\boldsymbol{g}_1^T, \boldsymbol{g}_2^T, ..., \boldsymbol{g}_K^T]^T = \boldsymbol{H}\ \boldsymbol{f} + \boldsymbol{w} \tag{2}$$

with $\boldsymbol{H} = [\boldsymbol{H}_1^T, ..., \boldsymbol{H}_K^T]^T$, $\boldsymbol{H}_i$ being the filter Toeplitz matrix with Toeplitz blocks associated to the PSF h_i expressed by:

[1]For simplicity, we adopted here a causal notation for the filters h_i.

$$\boldsymbol{H}_i = \begin{bmatrix} \boldsymbol{H}_i(0) & \cdots & \boldsymbol{H}_i(m_h-1) & & 0 \\ & \ddots & & \ddots & \\ 0 & & \boldsymbol{H}_i(0) & \cdots & \boldsymbol{H}_i(m_h-1) \end{bmatrix}$$

with

$$\boldsymbol{H}_i(n) = \begin{bmatrix} h_i(n,0) & \cdots & h_i(n,n_h-1) & & 0 \\ & \ddots & & \ddots & \\ 0 & & h_i(n,0) & \cdots & h_i(n,n_h-1) \end{bmatrix}$$

The objective of the considered image restoration problem is to find an estimate $\hat{\boldsymbol{f}}$ of the original image from observed images $\boldsymbol{g}_i$ using a maximum likelihood (ML) approach.

If we assume that the additive noise vectors $\boldsymbol{w}$ are white and Gaussian, then we can express the ML detection problem as the minimization of the squared Euclidean distance metric[2]:

$$\hat{\boldsymbol{f}} = \arg \min_{\boldsymbol{f} \in A} \|\boldsymbol{g} - \boldsymbol{H}\ \boldsymbol{f}\|_2^2 \tag{3}$$

where A represents the lattice associated to the gray level pixel values in the range $[0,\ 255]$. By applying a standard *QR* decomposition of the filter Toeplitz matrix $\boldsymbol{H}$, the previous least squares problem can be rewritten as:

$$\hat{\boldsymbol{f}} = \arg \min_{\boldsymbol{f} \in A} \|\boldsymbol{g}' - \boldsymbol{R}\ \boldsymbol{f}\|_2^2 \tag{4}$$

where $\boldsymbol{g}' = \boldsymbol{Q}^T \boldsymbol{g}$ and $\boldsymbol{R}$ is the square upper triangular matrix obtained from the previous QR decomposition.

III. Sequential Stack Decoder

A. Standard Stack Algorithm

The Stack algorithm is a tree search decoder that attempts to find a *best fit* using the observed blurred noisy images. In this section, we briefly introduce the steps of the Stack algorithm.

Before proceeding with the description of such an algorithm, we shall discuss the metric measure for the sequential decoding. It is basically based on the path metric M which is, at a k^{th} level of the tree, defined as:

$$M(\boldsymbol{f}^k) = \left\| \boldsymbol{g}'^k - \boldsymbol{R}_{kk}\ \boldsymbol{f}^k \right\|_2^2 \tag{5}$$

where $\boldsymbol{f}^k = [f_k, \ldots, f_2, f_1]^T$ denotes the last k components of the vector $\boldsymbol{f}$, $\boldsymbol{R}_{kk}$ is the lower k x k part of the triangular matrix $\boldsymbol{R}$, $\boldsymbol{g}'^k$ is formed by the last k components of $\boldsymbol{g}'$.

In the Stack algorithm, to determine a best fit (path) along the tree, a value is assigned to each node in the tree. This value is called the metric which is given by Eq. (5).

The mechanism of the Stack algorithm is described in the flowchart of Fig.1. To obtain the best and next best nodes, the Schnnor-Euchner enumeration [7] is used to generate nodes with metrics in ascending order. The decoding algorithm terminates when the top path in the stack reaches the end of the tree [8].

[2]This metric would be the l_1-norm if the noise is Laplacian.

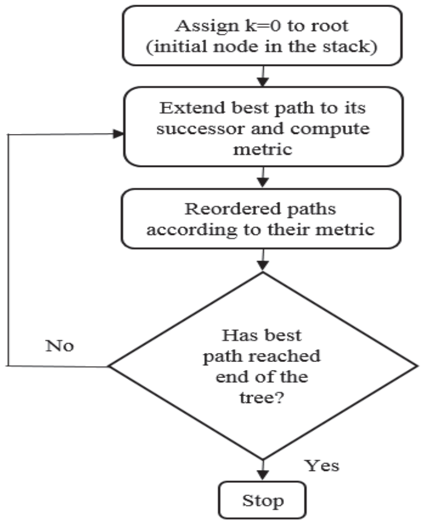

Fig. 1. Flowchart of the Stack decoding

The Stack decoder is applied on a d-ary tree with $d = 256$, where each node represents a value of the gray level of the image and each level of the tree represents a value of a pixel to estimate.

In summary, the algorithm steps are as follows:

- At the beginning, the stack contains only the root node of the tree (i.e., the empty path) with its path metric L_0 set arbitrarily to zero.
- A decoding operation consists to find the path S^i that corresponds to the metric L_i at the top of the stack, eliminating L_i from the stack, computing the metrics l_{i+1}^1, ..., l_{i+1}^d of the branches that leave the end node of the path S^i, and inserting the new path metric $L_{i+1}^i = L^i + l_{i+1}^i$, $i = 1, 2, ..., d$, into their proper positions according to size.
- The search ends when the decoder finds at the top of the stack a path whose length is equal to the size of the tree.

B. Improved Stack Algorithm

One of the major problems in image restoration is the algorithm's time complexity. Therefore, in this section we present a reduced cost version of the Stack algorithm. The proposed improvement is based on two main features, the structure of the convolution matrix $\boldsymbol{H}$ and the number of classes in the tree. These features are explained in details in the following:

1) Band Limited Matrix: As the convolution matrix $\boldsymbol{H}$ is band-limited, we obtain after the QR decomposition an upper triangular matrix $\boldsymbol{R}$ with a limited band (see Fig.2). In fact, the band size B of the triangular matrix $\boldsymbol{R}$ depends both on the size of the degraded image $[m_g\ n_g]$ and the convolution kernel $[m_h\ n_h]$, according to the following formula:

$$B = m_h\, n_h + (m_h - 1)\,(m_g - 1) \tag{6}$$

At this stage, when the least squares criterion are optimized, only the (B) non-zero elements are used in the matrix-vector product, this enables reducing significantly the computational cost as illustrated in section V.

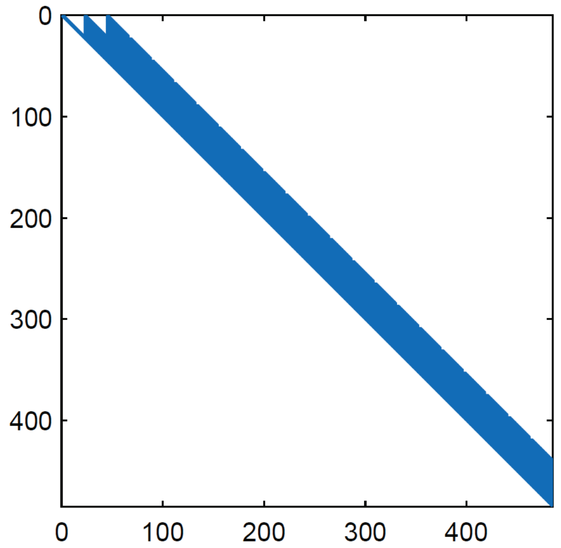

Fig. 2. Band Limited Matrix Structure

2) Hierarchical Approach: Instead of searching in the whole grayscale level range $[0,\ 255]$, the interval is divided into 2^N classes ($N < 8$). For each class we assign to the node the value of its center. Therefore, the tree search is done in two steps: gross and refined searches. Therefore, the branch metric to minimize per node becomes:

$$\hat{\boldsymbol{f}} = \arg \underset{f \in A}{min} \left\| \boldsymbol{g}' - \boldsymbol{R}\left(\boldsymbol{f}_G + \boldsymbol{f}_R\right)\right\|_2^2 \tag{7}$$

where $\boldsymbol{f}_G$ refers to the main image vector (which entries belong to the 2^N-length alphabet) while $\boldsymbol{f}_R$ is the refined component of the restored image taking values in a 2^{8-N} elements alphabet.

Step 1: a tree search is conducted considering the lattice associated to the 2^N classes

$$\hat{\boldsymbol{f}}_G = \arg \underset{f \in A_G}{min} \left\| \boldsymbol{g}' - \boldsymbol{R}\, \boldsymbol{f}_G \right\|_2^2 \tag{8}$$

Step 2: this step consists of refining our IR according to

$$\hat{\boldsymbol{f}}_R = \arg \underset{f \in A_R}{min} \left\| \hat{\boldsymbol{g}} - \boldsymbol{R}\, \boldsymbol{f}_R \right\|_2^2 \tag{9}$$

where $\hat{\boldsymbol{g}} = \boldsymbol{g}' - \boldsymbol{R}\, \hat{\boldsymbol{f}}_G$.

The resulting image of this hierarchical approach is given by the sum of the two estimated images

$$\hat{\boldsymbol{f}} = \hat{\boldsymbol{f}}_G + \hat{\boldsymbol{f}}_R$$

IV. The Regularization Model

In this section, we introduce in our system a regularization model that combines two approaches to restore images from blurry and noisy observations [9]:

- *Total variation (TV)* regularization is a technique that was originally developed by Rubin, Osher, and Fatemi (ROF) [10] for image denoising and deblurring. The TV regularization approach has been proven to be very effective in preserving sharp edges and object boundaries which are usually the most important features to recover.
- *Wavelet frame (WF)* regularization is a technique that ensures a full use of sparsity prior information and enables adaptive exploitation of the image regularity.

From Eq. (4) and under the combination of the discrete total variation and the wavelet transform regularizations, our model of restoration can be performed by the following minimisation problem:

$$\hat{\boldsymbol{f}} = \arg \underset{f \in A}{min} \left\| \boldsymbol{g}' - \boldsymbol{R}\, \boldsymbol{f} \right\|_2^2 + \alpha \left\| \boldsymbol{\nabla} \boldsymbol{f} \right\|_{TV} + \beta \left\| \boldsymbol{W} \boldsymbol{f} \right\|_1 \tag{10}$$

where $\boldsymbol{\nabla}$ is the discrete gradient, $\boldsymbol{W}$ is the discrete wavelet transform, $\|.\|_{TV}$ is a discrete TV norm, α and β are two positive regularization parameters that balance the three terms for minimisation and provides a trade-off between fidelity to measurements and noise sensitivity.

On one hand, for a given image $\boldsymbol{f} \in \mathbb{R}^{m_f \times n_f}$, the discrete gradient is defined as $\boldsymbol{\nabla f} = (\nabla_1 \boldsymbol{f}, \nabla_2 \boldsymbol{f})$, where ∇_1 and ∇_2 are two linear differential operators given by

$$\begin{cases} \nabla_1 f(i,j) = f(i+1,j) - f(i,j), & i = 1,..,m_f - 1 \\ & j = 1,..,n_f \\ \nabla_1 f(m_f,j) = f(1,j) - f(m_f,j), & j = 1,..,n_f \end{cases} \tag{11}$$

and

$$\begin{cases} \nabla_2 f(i,j) = f(i,j+1) - f(i,j), & i = 1,..,m_f \\ & j = 1,..,n_f - 1 \\ \nabla_2 f(i,n_f) = f(i,1) - f(i,n_f), & i = 1,..,m_f \end{cases} \tag{12}$$

The TV of f is defined as:

$$\left\| \boldsymbol{f} \right\|_{TV} = \sum \left\| \boldsymbol{\nabla f} \right\|_2 = \sum \sqrt{(\nabla_1 \boldsymbol{f})^2 + (\nabla_2 \boldsymbol{f})^2}$$

where $\sum$ denotes the sum taken over all pixels.

On the other hand, the wavelet transformation can be seen as a matrix-vector multiplication from a linear algebra point of view. The details about how to generate the WF transform are given in [11].

Note that the regularization terms in (10) do not have the appropriate form for a criterion optimization with the Stack algorithm. For this reason, we introduce the following approximations:

For the WF term, we replace the matrix $\boldsymbol{W}$ by $\boldsymbol{R_W}$, the upper triangular matrix given by the QR decomposition of $\boldsymbol{W}$. The TV-based regularization term is of the form $\|g(\boldsymbol{\nabla f})\|_2$ where g is an element-wise non-linear function and $\boldsymbol{\nabla}$ is an appropriate filtering matrix used for the horizontal and vertical gradient calculations in (11) and (12). Again, to fit the Stack algorithm structure, we replace the matrix $\boldsymbol{\nabla}$ by the upper triangular matrix $\boldsymbol{R_\nabla}$ obtained from its QR decomposition. In our simulations, we have observed that these modifications have only a little impact on the regularization performance.

V. Simulation Results

In this section, results of our proposed method based on the sequential Stack decoder are presented. For all experiments, images were generated by applying first the blur kernel on each of them and then adding additional Gaussian white noise with various standard deviations (STD). Moreover, the Peak Signal to Noise Ratio (PSNR) in dB and the Structural SIMilarity index (SSIM) were used for comparison purposes. SSIM index is shown to be a more reliable metric for comparison of restoration algorithms than the widely used PSNR measure [12].

$$PSNR = 10 \times \log \frac{255^2}{MSE} \, [dB] \tag{13}$$

$$SSIM = \frac{2\mu_f \mu_g + C1}{\mu_f^2 + \mu_g^2 + C1} \times \frac{2\sigma_{fg} + C2}{\sigma_f^2 + \sigma_g^2 + C2} \tag{14}$$

where MSE is the Mean-Squared-Error per pixel, (μ_f, μ_g) are the mean and (σ_f, σ_g) the variance of $\boldsymbol{f}$ and $\boldsymbol{g}$, respectively. (σ_{fg}) the covariance of $\boldsymbol{f}$ and $\boldsymbol{g}$. $C1$ and $C2$ are small constants set equal to 0.01 and 0.03, respectively.

A. Noiseless Case: Deblurring

In this subsection, we perform some numerical experiments in image restoration in the noiseless case. The original images (A: Cameraman (256×256)) and (C: Lena (512×512)) were here blurred using motion blur with the linear motion by 20 pixels in the direction of 45 degrees and Gaussian blur of size [3, 3] with standard deviation ($\sigma = 10$). The restored images are shown in Fig.3, where (A: $MSE = 1.0438$, $PSNR =$ 24.93 dB) and (C: $MSE = 4.9171$, $PSNR = 22.64$ dB) are the blurred images and (B) and (D) are their perfectly restored versions with MSE and SSIM equal respectively to 0 and 1 for both.

Fig. 3. (A)-(C): Blurred images, (B)-(D): Deblurred images with the Stack algorithm.

B. Noisy Case Multichannel IR

In this simulation, the original image (Cameraman (256×256)) was blurred by Gaussian blur ($\sigma = 1.5$) and then corrupted by a Gaussian noise with $SNR = 25$ dB.

First, Fig.4-A presents the restored image using our algorithm (without regularization) in the mono-channel case (A: $MSE = 0.1392$, $PSNR = 8.56$ dB, $SSIM = 0.1901$). The results of the restoration in the multichannel ($K = 3$) are presented in Fig.4-B (B: $MSE = 0.1060$, $PSNR = 9.7478$ dB, $SSIM = 0.5411$). The obtained results are clearly improved due to MC diversity which helps improving the conditioning of the matrix $\boldsymbol{H}$. However, the noise effect is still important and regularization is needed for a better IR.

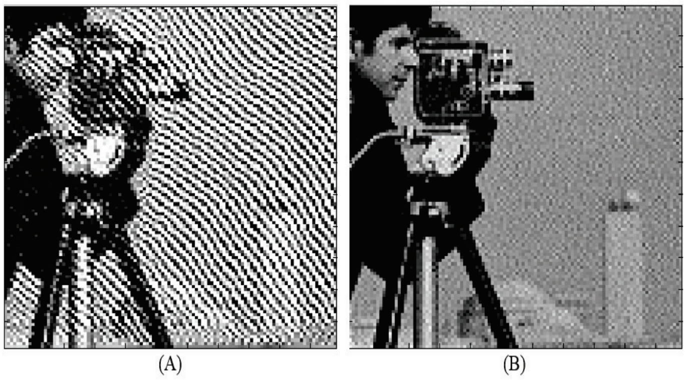

Fig. 4. (A): Mono-channel restored image, (B): Multichannel restored image.

C. The Need of Regularization

In this section, the obtained results using the two regularization terms (total variation and wavelet transform) are presented (Eq.10). First, the two regularization parameters (α and β), which control the trade-off between these terms and represent the amount of regularization, are set on an ad hoc basis to $1e^{-2}$ and $1e^{-1}$, respectively. Fig.5 shows the effects of regularization (without regularization-A: $MSE = 0.1060$, $PSNR =$ 9.7478 dB, $SSIM = 0.5411$) and (with regularization-B: $MSE = 0.1056$, $PSNR = 9.7644$ dB, $SSIM = 0.6019$). It's clear that the IR is improved. However, the algorithm's robustness to noise with dedicated regularization approaches has to be investigated further.

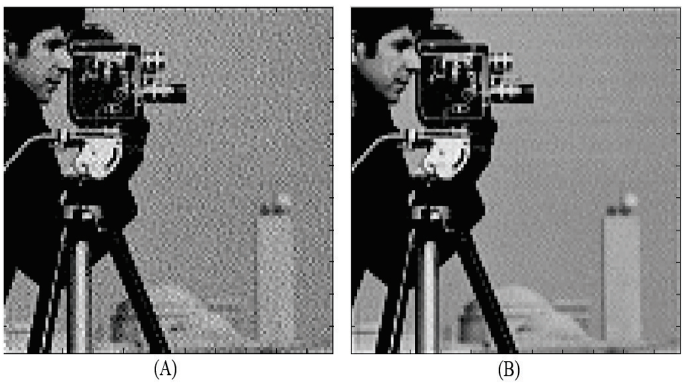

Fig. 5. (A): Restored image without regularization, (B): Multichannel restored image with regularization.

TABLE I
COMPARISON OF IMAGE QUALITY (SSIM) AND COMPUTING TIME (CT) FOR DIFFERENT SCHEMES

	SSIM	SSIM (%)	CT (s)	CT (%)
Stack	1	100	252.215	100
Stack (32 classes)	0.974	97.48	15.057	5.97
Stack (64 classes)	0.984	98.48	21.013	8.33

D. Improved Stack Algorithm

1) Band Limited (BL) Matrix: The Stack algorithm (with and without the exploitation of the band limited structure) was applied to a portion of the image (Cameraman (50×50)) blurred by a Gaussian blur of size [3, 3] and corrupted by a Gaussian noise. We run 100 Monte Carlo simulations of noise for different values of the Signal-to-Noise Ratio in the set $\{5, 10, 15, 20, 25, 30, 35, 40\}$dB. Fig.6 illustrates the computational cost gain of about 77% when we exploit the band limited structure of the triangular matrix $\boldsymbol{R}$.

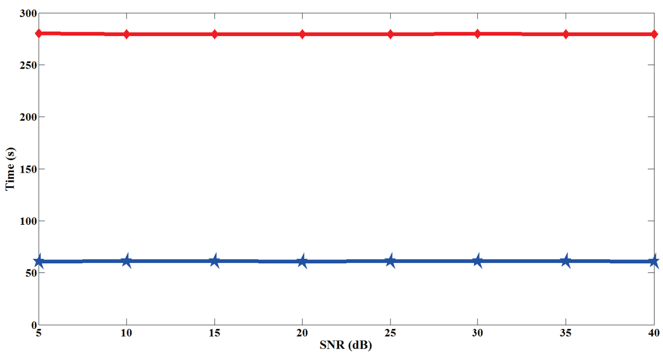

Fig. 6. Time Complexity of the Stack algorithm (without (red) and with (blue) use of BL structure)

2) Hierarchical Approach: This hierarchical approach is applied to images affected by three types of blur (Fig.7): motion blur with the linear motion by 3 pixels in the direction of 30 degrees and Gaussian blur of size [3, 3] with standard deviations ($\sigma_1 = 1.5$, $\sigma_2 = 5$).
Table I shows the little loss in quality of restoration (-1.52% for 64 classes, -2.52% for 32 classes) compensated by the huge gain in computational cost (-91.67% for 64 classes, -94.03% for 32 classes). An optimal choice for N (i.e. number of classes of the first step) combined with an enlarged search range interval for the refining stage (i.e. second step) is a potential source of additional improvement, currently under study.

VI. CONCLUSION

In this paper, we focused on a new technique for IR inspired from ML deconvolution in communication systems and based on the sequential Stack decoder. To reduce the computational cost, two approaches have been considered based on the BL structure of the filtering matrix and on a two-stage (hierarchical) restoration technique, respectively.

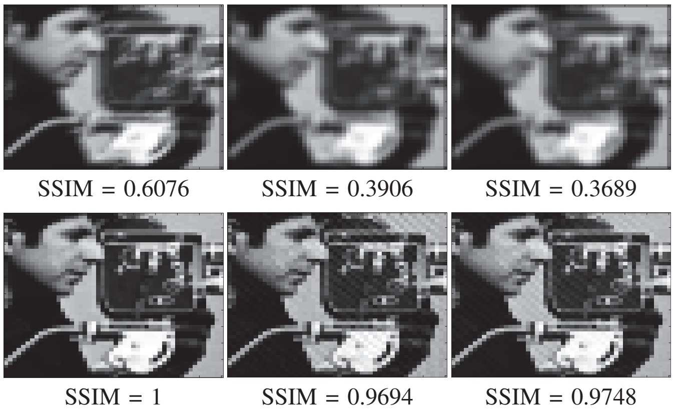

Fig. 7. IR with hierarchical approach with N=5. Blurred images (top) and original, gross and refined images (bottom from left to right).

In addition, to take into account the additive noise effect, appropriate regularisation terms have been added to the cost function. Finally, the paper provides numerical evaluations which reveal the good IR performance of the method and the significant computational cost reduction given by the proposed algorithm modifications.

REFERENCES

[1] A. C. Bovik, (ed.), *The essential guide to image processing*. Academic Press, 2009.
[2] J. Biemond, R. L. Lagendijk and R. M. Mersereau, *Iterative methods for image deblurring*. Proceedings of the IEEE, 1990, vol. 78, no 5, p. 856-883.
[3] W. Souidene, K. Abed-Meraim and A. Beghdadi, *A new look to multi-channel blind image deconvolution*. Image Processing, IEEE Transactions on, 2009, vol. 18, no 7, p. 1487-1500.
[4] M. O. Damen, H. EL Gamal and G. Caire, *On maximum-likelihood detection and the search for the closest lattice point*. Information Theory, IEEE Transactions on, 2003, vol. 49, no 10, p. 2389-2402.
[5] W. Abediseid and M. S. Alouini, *On lattice sequential decoding for the unconstrained AWGN channel*. Communications, IEEE Transactions on, 2013, vol. 61, no 6, p. 2446-2456.
[6] G. B. Giannakis and Jr. R. W. Heath, *Blind identification of multichannel FIR blurs and perfect image restoration*. Image Processing, IEEE Transactions on, 2000, vol. 9, no 11, p. 1877-1896.
[7] B. Hassibi and H. Vikalo, *On the sphere-decoding algorithm. part I: Expected complexity*. Signal Processing, IEEE Transactions on, 2005, vol. 53, no 8, p. 2389-2401.
[8] F. Jelinek, *Fast sequential decoding algorithm using a stack*. IBM Journal of Research and Development, 1969, vol. 13, no 6, p. 675-685.
[9] Q. Fan, D. Jiang and Y. Jiao, *A multi-parameter regularization model for image restoration*. Signal Processing, 2015, vol. 114, p. 131-142.
[10] L. I. Rudin, S. Osher and E. Fatemi, *Nonlinear total variation based noise removal algorithms*. Physica D: Nonlinear Phenomena, 1992, vol. 60, no 1, p. 259-268.
[11] A. Chai and Z. Shen, *Deconvolution: A wavelet frame approach*. Numerische Mathematik, 2007, vol. 106, no 4, p. 529-587.
[12] Z. Wang and A. C. Bovik, *Mean squared error: Love it or leave it? A new look at signal fidelity measures*. Signal Processing Magazine, IEEE, 2009, vol. 26, no 1, p. 98-117.